Mesoporous silica nanoparticles as a new carrier methodology in the controlled release of the active components in a polypill

Antonio L. Doadrio[a*], José M. Sánchez-Montero[b], Juan C. Doadrio[a], Antonio J. Salinas[a,c] and María Vallet-Regí[a,c*].

[a] *Departamento de Química Inorgánica y Bioinorgánica, Universidad Complutense de Madrid, Instituto de Investigación Sanitaria Hospital, 12 de Octubre i+12, Madrid, Spain.*

[b] *Departamento de Química Orgánica y Farmacéutica, Grupo de Biotransformaciones. Universidad Complutense de Madrid, Spain.*

[c] *Networking Research Center on Bioengineering, Biomaterials and Nanomedicine (CIBER-BBN), Madrid, Spain.*

***Corresponding authors:** María Vallet-Regí. Departamento de Química Inorgánica y Bioinorgánica, Facultad de Farmacia. Universidad Complutense de Madrid. 28040 Madrid. Spain. Email: vallet@ucm.es. Antonio L. Doadrio. Departamento de Química Inorgánica y Bioinorgánica, Facultad de Farmacia. Universidad Complutense de Madrid. 28040 Madrid. Spain. Email: antoniov@ucm.es

Abstract

Polypill is a medication designed for preventing heart attacks through a combination of drugs. Current formulations contain blood pressure-lowering drugs and others, such statins or acetylsalicylic acid. These drugs exhibit different physical chemical features, and consequently different release kinetics. Therefore, the concentration in plasma of some of them after the release process can be out of the therapeutic range. This paper investigates a new methodology for the control dosage of a polypill recently reported containing hydrochlorothiazide, amlodipine, losartan and simvastatin in a 12.5/2.5/25/40 weight ratio. The procedure is based on Mesoporous Silica Nanoparticles (MSN) with MCM-41 structure (MSN-41) used as carrier, aimed to control release of the four drugs included in the polypill. *In vitro* release data were obtained by HPLC and the curves adjusted with a kinetic model. To explain the release results, a molecular model was built to determine the drug-matrix interactions, and quantum mechanical calculations were performed to obtain the electrostatic properties of each drug. Amlodipine, losartan and simvastatin were released from the polypill-MSN-41 system in a controlled way. This would be a favourable behaviour when used clinically because avoid too quick pressure decrease. However, the diuretic hydrochlorothiazide was quickly released from our system in the first minutes, as is needed in hypertensive urgencies. In addition, an increase in the stability of amlodipine and hydrochlorothiazide occurred in the polypill-MSN-41 system. Therefore, the new way of polypill dosage proposed can result in a safer and effective treatment.

Keywords: Polypill, MCM-41 nanoparticles, antihypertensive drugs, cholesterol lowering, diuretic.

Chemical compounds studied in this article

Hydrochlorothiazide (PubChem CID: 3639); Amlodipine besylate (PubChem CID: 60496); Losartan potassium (PubChem CID: 11751549); Simvastatin (PubChem CID: 54454).

Abbreviations

MSN, mesoporous silica nanoparticles; MSN-41, mesoporous silica nanoparticles with MCM-41 structure; MCM-41, Mobil composition of matter #41; MCM-41s, Mobil composition of matter #41 simplified molecular model; CVD, cardiovascular diseases; ESC, European Society of Cardiology; HTZ, hydrochlorothiazide; AML, amlodipine; LS, losartan; SV, simvastatin; EtOH, ethanol; BET, Brunauer, Emmett and Teller method; BJH, Barret-Joyner-Halenda equation; PSA, polar surface area; DM, dipole moment; ADME, absorption, distribution, metabolism, and excretion.

1. Introduction

Cardiovascular diseases (CVD) are the leading cause of death worldwide (Castelli et al., 1986; Gordon et al., 1977; Kannel and McGee, 1979; Mitchell et al., 2010; Wilson et al., 1998). Hypertension is an important risk factor for CVD. Thus, in those patients already having a cardiovascular problem, hypertension can intensify the damage (Collins et al., 1990; Ford et al., 2007; MacMahon et al., 1990). Current hypertension therapies display two key problems. First, the majority of hypertensive treatments need to take daily several drugs (Chobanian et al., 2003; D'Amico et al., 1998; James et al., 2014). Therefore, if the patient could forget to take some of the doses, decreasing the safety and increasing the side effects of hypertension. Second, too quick or too slow decreases in blood pressure produce is undesirable. Thus, an excessively rapid decrease may result in hypoperfusion of central nervous system with can yield to stroke, paraplegia, blindness or death. On the other hand, a very slow decrease is ineffective in hypertensive emergencies. Due to these facts, the maximum recommended blood pressure drop by 25% within the first two hours of treatment to reach 160/100 mmHg after six hours and then to the normal blood pressure levels in the following hours or days.

To avoid possible inadvertences of the patient in taking medication doses, the multi-target drugs design proposes a systemic solution, safer and with lower side effects. Thus, medications containing several active components in a single dose (Bender et al., 2006; Bolognesi, 2013; Petrelli and Valabrega, 2009) that for hypertension treatment is called polypill (Lonn et al., 2010; Sleight et al., 2006; Study, 2009). For instance, Laboratorios Ferrer (Spain) commercialized Sincronium® and Trinomia® polypill containing acetylsalicylic acid to prevent heart attacks, ramipril, an angiotensin-converting enzyme inhibitor, and simvastatin or atorvastatin, as cholesterol lowering drugs. To reach the suitable blood pressure reduction rate, an effective controlled release of the drugs is required, which seems unlikely in the polypill currently commercialized with a conventional formulation. Thus, new research approaches are required in this field. In this sense, MSN-41was investigated as effective carrier for the controlled local release of individual active ingredients (Colilla et al., 2013; Knežević et al., 2013; Ruiz-Hernandez et al., 2011; Slowing et al., 2008; Tang et al., 2012; Vallet-Regí et al., 2007; Vallet-Regi et al., 2001) but not for a polypill.

On the other hand, several hypertension guidelines recommend the inclusion in the treatment of a diuretic like hydrochlorothiazide (HTZ) e.g. European Society of Cardiology guidelines (ESC, June, 2016). In this regards, the combination of HZT and amlodipine (AML), a calcium channel blocker, with an angiotensin inhibitor, such as benazepril, ramipril or losartan (LS), is very effective to decrease the rate of cardiovascular events (Jamerson et al., 2008). Moreover, if the polypill containing a cholesterol lowering drug, it can be reduced by 80% the risk of CVD in patients with vascular disease (Chrysant and Chrysant, 2014; Exaire-Murad et al., 2015; Gadepalli et al., 2014; Katsiki et al., 2013; Wald and Law, 2003; Yusuf, 2002). Likewise, in a prevention trial of a polypill composed by AML, LS, HTZ, and simvastatin (SV), the mean systolic blood pressure was reduced by 12%, the diastolic blood pressure by 11%, and low-density lipoprotein (LDL) cholesterol by 39% (Wald et al., 2012).

In the present work, we investigated, for the first time, the capability of a nanocarrier, based on MSN-41 silica nanoparticles, to host and release the four active components: HTZ, AML, LS and SV in 12.5/2.5/25/40 wt-ratio, contained in a polypill previously reported (Wald et al., 2012) according with the National Center of Biotechnology Information (NCBI). The objective was to reach a controlled release and a higher stability of the drugs to improve the traditional pharmaceutical formulation. For this purpose, analytical methods, molecular modelling and docking analysis were used as described elsewhere (Doadrio et al., 2010; Doadrio et al., 2014).

2. Experimental

2.1. Synthesis of MSN-41 mesoporous material

Synthesis of MSN-41 with hexagonal pore arrangement, was performed by sol-gel in the presence of structure directing agents and following a modified Stöber method (Stöber et al., 1968). Hence, to a 1L round-bottom flask, 1g of cetyltrimethyl-ammonium bromide (CTAB, Sigma-Aldrich, Spain) as a structure-directing agent, 480 mL of H_2O (Milli-Q) and 3.5 mL of NaOH (2 M) were added. The mixture was heated at 80 ºC and stirred at 600 rpm. When the reaction mixture was stabilized at 80 ºC, 5 mL of tetraethyl-orthosilicate (TEOS, Sigma-Aldrich, Spain) were added dropwise at 0.33 mL/min. The suspension obtained was stirred further 2 h at 80 ºC. After filtration and washing with water and ethanol, the surfactant was removed by extraction with a NH_4NO_3 (Sigma-Aldrich, Spain) solution (10 mg/mL) in ethanol (EtOH) 95%. Finally,

the product was filtered and washed 3 times with 100 mL of H_2O and with 50 mL of EtOH and dried under vacuum at 40 ºC.

2.2. Drug-MSN-41 samples loading

We prepared five different drug-MSN-41 samples. Samples 1 to 4 are the result of loading each drug in MSN-41. Sample 1 (HZT-MSN-41) was hydrochlorothiazide (99.25% purity)-MSN-41; sample 2 (AML-MSN-41) was amlodipine besylate (100% purity)-MSN-41; sample 3 (LS-MSN-41) was losartan potassium (99.80% purity)–MSN-41 and sample 4 (SV-MSN-41) was simvastatin (100% purity)-MSN-41. Sample 5 was the result of the polypill containing the four component simultaneously loaded in MSN-41 (polypill-MSN-41). Polypill was prepared using a mixture of HTZ, AML besylate, potassium LS and SV in a 12.5/2.5/25/40 weight ratio. Normon Laboratories, Madrid, Spain, supplied all these products.

Samples were prepared dissolving: HTZ, 50 mg; AML, 10 mg; LS 100 mg and SV 160 mg (separately or together in the polypill) in 20 mL EtOH. Thereafter, 400 mg of MSN-41 were added with stirring for 24 h at room temperature for loading. After filtration, samples were dried in a vacuum oven at 20 ºC for 24 h.

The loading process was always performed following the protocol described, which guaranteed its reproducibility. Furthermore, measurements were performed in triplicate and the indicated values correspond to the average of three measurements.

The concentration of drug adsorbed in each MSN-41 sample (C_a) was obtained by the equation:

$$C_a = C_i - C_r \quad (1)$$

where C_i is the initial concentration before loading i.e. HTZ, 2.5; AML, 0.5; LS 5 and SV 8 in mg/mL and C_r is the concentration analysed by HPLC in the residue of the drugs adsorption on MSN-41. From these data, was estimated the % of adsorption for each drug.

2.3. HPLC method

RP-HPLC (Reversed Phase High Performance Liquid Chromatography) measurements were performed with a liquid chromatographic system equipped with a Waters Alliance 2695 separation module (Waters, Milford, Massachusetts, USA), a variable-wavelength diode array detector Waters 2996 and controlled by Millennium 32 software. A Zorbax Eclipse XDB-C-18 reversed-phase column (5 µm, 4.6 x 150 mm), supplied by Agilent Technologies, USA, was employed operating at 40 ºC. The mobile

phase was acetonitrile/Sörensen buffer at pH 3.5 (v/v) in a concentration gradient showed in Table 1. The flow rate was 1 mL/min. The effluent was monitored at 254 nm for HTZ and at 234 nm for LS, AML and SV. The injection volume was 10 μL. In these conditions, the retention times (t_r) for HTZ, AML, LS and SV were 1.79, 2.61, 4.45 and 15.8 min, respectively. Four-calibration curves using the standard drugs loaded in MSN-41 were plotted using concentrations in methanol for each drug of 0.1, 0.5, 1 and 1.5 mg/mL.

2.4. Characterization

Samples were characterized by powder X-ray diffraction (XRD), Fourier transform infrared (FTIR) spectroscopy and N_2 adsorption-desorption. The XRD patterns were obtained in a Philips X´Pert MPD (Cu Kα radiation) diffractometer. The diffractograms were collected in the 2θ range of 0.6–10º with a step size of 0.02º. FTIR spectra were recorded with a Nicolet Nexus spectrophotometer in the range of 4000–400 cm^{-1} by using a ATR golden gate accesory. The surface area and pore size of the materials were determined by N_2 adsorption using a Micromeritics ASAP 2020 porosimeter. Previously, loaded samples were degassed at 100 ºC for 24 h under vacuum (1.3 Pa). The pore size distribution was calculated from adsorption branches of the nitrogen isotherms using the Barret-Joyner-Halenda (BJH) equation (Barrett and Joyner, 1951) and the BET surface area was calculated by Brunaver, Emmett and Teller method (Brunauer et al., 1938). Furthermore, the particle morphology was analysed by scanning electron microscopy (SEM) using a Hitachi S-350 JSM 6335F field emission microscope operated at 20 kV. Finally, high-resolution transmission electron microscopy (HRTEM) was carried out with a JEOL 3000 FEG electron microscope operating at 300 kV (Tokyo, Japan). TEM images were recorded using a CCD camera (MultiScan model 794, Gatan, 1024 × 1024 pixels, size 24 μm × 24 μm).

2.5. MSN-41 samples release

The drug-loaded MSN-41 samples (1 to 5) were soaked in 20 mL of Sörensen phosphate buffer at pH= 7.5 (compatible with biological pH) and maintained at 37 ºC with stirring for all the assay time. The drugs concentration in solution was measured by HPLC as described above.

For kinetic analysis we have used the Peppas equation (Ritger and Peppas, 1987): $M_t/M_\infty=kt^n$, being M_t/M_∞ the drug-released fraction at time t and k reaction rate

constant, to know the drugs release mechanism governed by n. Thus, a value of n = 0.5 indicates a Fickian diffusion, while n values < 0.5 indicate the presence of other simultaneous processes. For n = 0.5, the Higuchi equation (Higuchi, 1963) based on the Fick's law can be used. However, when n is < 0.5, as it happens in this study, controlling release mechanisms were investigated according to non-lineal exponential proportional rate growth or decrease model and the best-fit curve using Origin v.9 software (OriginLab® Northampton, USA.). The kinetic model is given as:

$$D_{(t)} = A(1-e^{-kct\ -vc}) \quad (2)$$

where $D_{(t)}$ is % of drug released for each sampling time, A is the asymptote, c and v are adjustment parameters, k is the kinetic constant observed and t is the time in min^{-1}. The model, a non-lineal first-order kinetic, resulted in the most precise adjustment for this study.

On the other hand, highest percentage of drug released ($\%D_{max}$) was obtained by the equation:

$$\%D_{max} = C_{tmax}*100/C_a \quad (3)$$

where C_{tmax} is the concentration of each drug measured by HPLC at t_{max} and C_a is defined by Eq. (1). The maximum times (t_{max}) was when the drug degradation for each drug started at the pH of the study (7.5). The drug degradation starts when the measured drug concentration decrease.

To check that the silica dissolution do not influence the drugs stability, for each drug we performed a study by HPLC in identical conditions of a MSN-free system.

Finally, the percentage of drug released at 5 min ($\%D_5$) was obtained by the equation:

$$\%D_5 = C_5*100/C_{tmax} \quad (4)$$

where C_5 is the concentration of each drug measured by HPLC at 5 min and C_{tmax} is defined by Eq. (3). The time at 5 min corresponds to the first fast desorption process that occurs in the drugs studied and will be described in section 3.3.1.

2.6. Molecular modelling

A simulated MCM-41 molecular model was generated by using the Hyperchem 8.01 software (Hypercube, Inc. Gainesville, FL). The building unit in this model was the pseudo-cell, Si_6O_{12}, consisting of hexagonal arrangements of Si–O–Si units. The oxygen atoms saturate all the silicon atoms at the pore surface. Furthermore, hydrogen atoms saturate the oxygen atoms bonded to less than two silicon atoms. Therefore, all

the hydroxyl groups are located at the outer surface of the model. From this 2D layer structure, the 3D model was generated by using the built module of Hyperchem software. That way, 15 layers were added until reaching a model of 7.03 nm length and 2.1 in diameter. The final structure was refined by optimization of the geometry using the 500 steps of Stepest-Descend and 1500 steps Polak-Ribiere conjugate gradient algorithms both using the MM+ force field. The minimization process concluded when the energy converged or when a gradient of 0.1 kcal/mol was reached.

However, for docking calculations, the size of MCM-41 model exceeds the operating capability of our system. In consequence, an AM1 semi-empirical method for a simplified MCM-41 model of 8 layers with dimensions 2.10 nm of diameter and 3.81 nm length (MCM-41s) was used. HTZ, AML, LS, and SV docking calculations on the MCM-41s model surface were carried out by using ArgusLab 4.0.1 software with a cubic box of 6 nm x 2.7 nm x 2.7 nm and grid resolution of 0.040 nm. The binding site was defined from the ligands coordinates in the MCM-41s model. Argusdock exhaustive search docking engine was used (Morris et al., 1998). All calculations were made in vacuum due to the construction of a solvent box not change substantially the results. Therefore, these calculations adding complexity to the system by increasing the calculation time.

For electrostatic potential maps, coordinates of HTZ, AML, LS and SV drugs were obtained from DrugBank v. 5.0 (DrugBank, June, 2016) and treated by molecular dynamics simulations from Spartan´14 (Wavefunction, Inc.). Area, volume, polar surface area (PSA) and dipole moment (DM) of HTZ, AML, LS and SV molecules were also obtained, which are shown in Table 2.

3. Results and discussion

3.1. Samples characterization

Samples as received by different experimental techniques were characterized. Fig. 1 shows SEM and TEM images of sample 5 after the release process. As is observed by SEM, the MSN-41 particles maintained their spherical shape with average diameter close to 150 nm in a quite homogeneous size distribution. Furthermore, the heterogeneities observed in TEM micrograph are indicative of the partial loss of the 2D-hexagonal arrangement of MSN-41. This finding can be explained considering a partial dissolution of the silica network that would happen during the drugs loading (24 h in

ethanol) and the release (196 h in phosphate buffer at pH 7.5) processes. These results would agree with the reported *in vitro* degradation of mesoporous silica networks after being soaked by 240 h in different aqueous media (Izquierdo-Barba et al., 2010). In this case, the partial dissolution of the nanoparticles is not relevant for the loading and the final drug formulations because the time of drug degradation is lower that the dissolution time. In addition, the degradation times of the four drugs were identical in MSN-free and MSN-containing systems.

Fig. 2 shows Low Angle-XRD patterns and N_2 adsorption-desorption isotherms (inside) of MSN-41 and sample 5 after releasing. MSN-41 pattern shows three diffraction maxima at 2.05º, 3.7º and 4.3º in 2θ, which can be respectively indexed to (10), (11) and (20) reflections of a 2D hexagonal arrangement, being the unit cell parameter a_0= 4.98 Å. For sample 5 the XRD pattern shows only a diffuse shoulder indicating the partial loss of mesoporous order with the simultaneous inclusion of the four drugs in the nanoparticles. This inclusion nearly fills the mesopores of the nanoparticles. In addition, the electrostatic interactions and by hydrogen bond between the drugs with the matrix are intense, what causes strains within pores that can deform the pore wall and consequently the pore shape. An analogous deformation of the mesopores was reported after the functionalization of a mesoporous matrix. (Doadrio et al., 2014).

The isotherms shape with absence of hysteresis cycle indicates that the pores size is enough small to avoid the N_2 molecules condensation. These are the typical curves of MCM-41 materials with cylindrical pores of small size. From these measurements was obtained a maximum in the diameter of pore (D_p) of 4.64 nm and BET surface area (S_{BET}) of 1047.6 m^2/g for MSN and 2.0 nm (D_p) and 289.5 m^2/g (S_{BET}) for polypill-MSN-41. XRD patterns and N_2 adsorption-desorption isotherm results are consistent with the entrance of drugs into matrix mesopores.

Finally, the FTIR characterization of MSN-41 and polypill-MSN-41 exhibited quite similar spectra dominated by the presence of the three bands characteristic of MCM-41 silica at 1050-1057 cm^{-1}, 954 cm^{-1}, 800-804 cm^{-1} and 439 cm^{-1} (results not shown).

3.2. Samples adsorption

The C_a values obtained for samples 1 to 4 by using Eq. (1) were: HTZ, 1.25; AML, 0.24; LS, 2.03 and SV, 3.9 in mg/mL, respectively and essentially the same were

found for sample 5. Therefore, the adsorption of drugs was close to 50%, that is, HTZ= 50±0.5%, AML= 48±0.5%. SV= 48.8±0.5%, and somewhat lower for LS that was 41±0.5%.

3.3. Samples release

As it is established, the drug released from ordered mesoporous materials such as MCM-41 take place through a Fickian diffusion mechanism (Vallet-Regí et al., 2007; Yang et al., 2012). In these cases, normally the Higuchi equation can be applied. However, in this study, the values of n obtained from Peppas equation were lower than 0.5, indicating the existence of other processes that influences the drug release. For this reason, we used the nonlinear first order Eq. (2), which includes most of the factors involved in the drug release rate. This adjustment is better than those accomplished with the classical Higuchi equation. For example, for HTZ-MSN-41 (sample 1) with n= 0.49 (maximum value reached for a sample), when applying Higuchi equation, the R^2 obtained was 0.23 while with the Eq. (2) was 0.956. Analogous results were obtained for the other samples with values of n lower than 0.49.

It must be considered that in the release of a drug from a mesoporous matrix two stages take place. The one, a fast desorption, when the material is filling with water, leads to an uncontrolled drug release. The second one, which takes place when pores are already filled, results in a controlled drug release. The first stage mainly depends on the solubility of the drug in water. The second one is more complex and involves many factors. Among them, the electrostatic interactions, hydrogen bonds, as well as solid-liquid diffusion, such as the area, volume, polarity (including PSA and DM), as well as liposolubility, percentage of ionization (pKa-pH), lipophilicity (log P), tortuosity of the channels, and the drug solubility (Doadrio et al., 2015). On the other hand, previous articles demonstrated that hydrogen bond and electrostatic forces factors could be critical in the release of a drug from the mesoporous matrix (Doadrio et al., 2010; Doadrio et al., 2014).

3.3.1. Samples 1-4 controlled release

First, for comparative purposes, we studied the release of HTZ, AML, LS and SV, independently loaded on MSN-41 (samples 1 to 4). Kinetic data, including the n parameter, observed kinetic constants (K_{obs}) and R^2 for each drug-MSN-41 are shown in

Table 3. Additionally, in Table 3 shows the values obtained of $\%D_{max}$ and $\%D_5$ from Eq. 3 and Eq. 4, respectively, besides t_{max}.

Considering first the kinetic rate constants (K_{obs}) in samples 1 to 4, respectively. For HTZ in sample 1, K_{obs} is bigger (0.51) than in the other three samples: AML in sample 2 (0.0016), LS in sample 3 (0.001) and SV in sample 4 (0.0044). Consequently, HTZ release is faster than those of other drugs.

Moreover, the profile of the release curve for sample 1 shows a sudden release of HTZ in the first 5 min of assay. Analogous behavior was observed for samples 2 to 4, but with a slower release profile (Fig. 3). This corresponds to the first stage in the drug release mechanism previously mentioned. For a controlled release, the drug desorption rate must be constant over a period. This does not occur during the first stage of drug desorption, but it occurs during the second stage. Therefore, to reach a controlled release of a drug from MSN-41 it is necessary a relatively insignificant desorption (in time and weight) on the first stage. This happens for AML-MSN-41, LS-MSN-41 and SV-MSN-41 but not in HTZ-MSN-41. For HTZ-MSN-41, an 80.5 % was released in the first 5 min ($\%D_5$), while in AML-MSN-41, LS-MSN-41 and SV-MSN-41, the release process is controlled from the outset, with $\%D_5$ values of 6.6, 3.3 and 6.0%, respectively. This can be explained by the different solubility of the drugs in water. That way, HTZ had a high desorption in the first stage, because it dissolves rapidly in water (722 mg/mL at 25 ºC), in contrast with AML (75 mg/mL), LS (0.8 mg/mL) and SV (< 0.8 mg/mL) (PubChem, June, 2016). In addition, the polarity of drugs should be taken into account (Table 2). In this sense, a polar molecule such as HTZ should have more affinity for water with respect to AML, LS and SV.

In the AML, LS and SV release the prevalent factor is log P. The most lipophilic molecule investigated is SV (log P= 4.7), thus is the most retained drug with respect to AML (log P= 3.0) and LS (log P= 4.3) (PubChem, June, 2016). However, the release rate of AML and LS are similar. This confirms that there is not a rapid desorption of AML, LS and SV, because the release process is controlled from the beginning. In these cases, other parameters exert their action from the outset influencing the control of delivery from MSN-41.

Another factor that should influence the release of AML, LS and SV on MSN-41 is pKa. The pKa values for these drugs are AML, 8.79; LS, 5.5 and SV, 14.9 (PubChem, June, 2016). For these values, the % ionization obtained by Henderson-Hasselbalch equation was: 4.89 for AML, 99.0 for LS and only 4.10^{-6} for SV. These data suppose

that SV will be primarily in its neutral form, while LS will be ionized. Besides, SV is the least soluble, which agree with a neutral form. LS is also very sparingly soluble but it is ionized, which increase its solubility and AML is more soluble than those two. The lipophilicity of the SV makes to be less retained in the mesoporous matrix than AML and LS.

3.3.2. Polypill-MSN-41 controlled release

Then, we have studied our polypill-MSN-41 (sample 5) and the kinetic results are shown in Table 4. In this sample, there are interactions among the components of the polypill. This fact was demonstrated from docking calculations in the simplified MCM-41s model (Fig. 4a) where interactions among four-drug molecules were observed (Fig. 4b). Furthermore, molecular modeling calculations showed that drug molecules exhibit negatively charged areas and other areas of positive charge, so London electrostatic interactions between them are possible (Fig. 4c). In addition, all molecules have the possibility to join by hydrogen bonds between them and with the matrix.

All these facts influence the desorption results of the drugs. Thus, there is a major release of the total amount of the polypill components. For instance, HTZ it released 14.7 times more in the polypill-MSN-41 ($\%D_{max}$= 9.88) than in HTZ-MSN-41 (0.67). The same happens for AML, 1.72 times (22-12%); LS, 1.28 times (1.1-0.85%) and SV, 3.68 times (0.14-0.038%).

On the other hand, release profiles do not change substantially (Fig. 3) in the polypill-MSN-41 (sample 5), with a rapid desorption on the first 5 min for HTZ ($\%D_5$, 82.9) similar to HTZ-MSN (sample 1), but with better control for AML (2.6-6.6%), LS (1.6-3.3%) and SV (3.5-6.0%). These facts indicate a controlled release in the polypill-MSN-41 for AML, LS and SV, but not for HTZ, as it happened in sample 1 (HTZ-MSN-41). However, this behavior would be beneficial for HTZ, a drug used in hypertensive emergencies. In addition, K_{obs} values of HTZ, AML, LS and SV in sample 5, i.e. 0.49, 0.0011, 0.0022 and 0.0017, respectively (Table 4), are consistent to those obtained with the drugs separately loaded, although LS is higher while SV is lower (Table 3).

Consequently, all these findings clearly evidence that there are many factors related to drug adsorption/resorption processes. As a result, the proposed model in this paper based on a non-linear first-order kinetic was the appropriate.

3.3.3. Drug stability

The polypill-MSN-41system has improved the drug stability. Thus, in all cases, the time of drug stability is larger than required for its metabolization (1 to 5 h). Furthermore, HTZ, AML, LS and SV are stable in our system until 48, 98, 170 and 48 h, respectively. These values are higher than those of the drug half-life, which range: 5.6-14.8 h for HTZ, 30-50 h for AML, 2 h for LS and 3 h for SV (DrugBank, June, 2016). Moreover, HTZ and AML are higher stable than when each drug was loaded separately in MSN-41 matrix. Thus, HTZ in sample 1 only was stable until 32 h and AML until 48 h. These results can be attributed to the interaction observed by docking between AML and HTZ. The increase in the drug stability will be especially important in the pharmaceutical application of AML, LS and SV because the antihypertensive and cholesterol lowering medication requires a chronic treatment. Identical degradation times for the four drugs were obtained in MSN-free polypill systems.

3.4. Molecular modelling

In order to understand the release mechanism of polypill-MSN-41 a new MCM-41 model was built with a hexagonal channel of the MCM-41 matrix of greater length. This new structure is formed by 2D hexagonal mesopore where the walls are composed by amorphous silica. Fig. 5 shows the model obtained by molecular modelling. Models of silica mesopores specifically for MCM-41, have been designed by our group (Doadrio et al., 2010; Doadrio et al., 2014) and other authors (Coasne and Ugliengo, 2012; He and Seaton, 2003; Ugliengo et al., 2008; Williams et al., 2016; Zhuo et al., 2008). However, these MCM-41 models were built with the purpose of introducing a single molecule into the matrix or without and has not been tested with four molecules at a time. Besides, the small length of the channels previously used prevented a realistic view about the molecules and molecules-matrix interactions in four drugs models. In this way, the new MCM-41 model designed with larger pore diameter and length is more realistic allowing introduce four drug.

Docking studies confirm that the four molecules studied can penetrate by size and electrostatic charge in the tested MCM-41 model and that HTZ and AML can join together by electrostatic forces (Fig. 4). Another possibility is that the molecules of other components of the polypill also join each other. This is in agreement with LS being retained significantly lower in the polypill-MSN-41 (sample 5) and the SV being

more retained. The interaction energies of the four molecules with the matrix calculated by molecular docking were: AML: -3.6 Kcal/mol; LS: -4.17 Kcal/mol; SV: -4.24 Kcal/mol and HTZ: -4.18 Kcal/mol. Moreover, docking showed the charge compatibility between the four-drug and with the mesoporous silica matrix. On the other hand, docking calculations did not allow us to calculate the interactions between the drug molecules. From the values of the dipolar moments showed on Table 2 it can be deduced that HTZ is the most polar of the four components of the polypill with a dipolar 9.15 D. On the contrary, AML show the lower dipolar moment with a value of 1.87 D. Moreover, the right part of Figure 4 shows the images the electrostatic potential of the four molecules. As it is observed, AML shows a strongly positive region, not present in the other molecules. This region can strongly bond with the highly negative region of HTZ and would explain the interaction between both molecules.

The polypill-MSN-41 system could be administered as coated tablets or by parenteral way; the last one not affected by the intestinal absorption. Moreover, to determine the pharmacologically active doses of drugs released and the ADME (absorption, distribution, metabolism, and excretion) process, in vivo pharmacokinetic and pharmacological studies will be needed.

4. Conclusions

This study has shown that MSN-41 mesoporous silica nanoparticles, can be an effective carrier for a polypill dosage. This carrier, allows an effective controlled release of AML, LS and SV and a quick release of HTZ. A controlled release of AML and LS ensures the proper metabolization in antihypertensive treatment, discarding the adverse effects of a too higher or too lower dose. Furthermore, the controlled release of SV is suitable for long-term treatments. Moreover, the quick release of HTZ from polypill-MSN-41 will be optimum for hypertensive emergencies treatment.

In addition, MSN-41 carrier increase the stability of the four components of the polypill investigated improving their half-life and metabolism time. Moreover, HTZ and AML are more stable in the polypill that when were released independently from MSN-41 because a bond between both molecules by electrostatic forces is established.

The MCM-41molecular model built in this study confirmed the release results obtained by HPLC.

Therefore, a new approach for the dosage of a polypill has been opened in this study that can result in a safer and effective treatment.

Acknowledgments

Financial support of Ministerio de Ciencia e Innovación (MICINN) Spain, through the project MAT2015-64831-R and Ministerio de Economía y Competitividad through the Spanish and European Network of Excellence CSO2010-11384-E and the FIS project PI15/00978 are acknowledged. Normon Laboratories by the principles active supply and Dr. Manuel Cordoba by helpful discussions of the kinetic results are also acknowledged.

References

Barrett, P., Joyner, L., 1951. PP Halenda The determination of pore volume and area distributions in porous substances–Computations from nitrogen isotherms J. Am. Chem. Soc 73, 373-380.

Bender, A., Jenkins, J.L., Glick, M., Deng, Z., Nettles, J.H., Davies, J.W., 2006. "Bayes affinity fingerprints" improve retrieval rates in virtual screening and define orthogonal bioactivity space: when are multitarget drugs a feasible concept? Journal of chemical information and modeling 46, 2445-2456.

Bolognesi, M.L., 2013. Polypharmacology in a single drug: multitarget drugs. Current medicinal chemistry 20, 1639-1645.

Brunauer, S., Emmett, P.H., Teller, E., 1938. Adsorption of Gases in Multimolecular Layers. Journal of the American Chemical Society 60, 309-319.

Castelli, W.P., Garrison, R.J., Wilson, P.F., Abbott, R.D., Kalousdian, S., Kannel, W.B., 1986. Incidence of coronary heart disease and lipoprotein cholesterol levels: The framingham study. JAMA 256, 2835-2838.

Chobanian, A.V., Bakris, G.L., Black, H.R., Cushman, W.C., Green, L.A., Izzo Jr, J.L., Jones, D.W., Materson, B.J., Oparil, S., Wright Jr, J.T., 2003. The seventh report of the joint national committee on prevention, detection, evaluation, and treatment of high blood pressure: the JNC 7 report. Jama 289, 2560-2571.

Chrysant, S.G., Chrysant, G.S., 2014. Future of polypill use for the prevention of cardiovascular disease and strokes. The American journal of cardiology 114, 641-645.

Coasne, B., Ugliengo, P., 2012. Atomistic Model of Micelle-Templated Mesoporous Silicas: Structural, Morphological, and Adsorption Properties. Langmuir 28, 11131-11141.

Colilla, M., González, B., Vallet-Regí, M., 2013. Mesoporous silica nanoparticles for the design of smart delivery nanodevices. Biomaterials Science 1, 114-134.

Collins, R., Peto, R., MacMahon, S., Godwin, J., Qizilbash, N., Hebert, P., Eberlein, K., Taylor, J., Hennekens, C., Fiebach, N., 1990. Blood pressure, stroke, and coronary heart

disease: part 2, short-term reductions in blood pressure: overview of randomised drug trials in their epidemiological context. The Lancet 335, 827-838.

D'Amico, G., Pagliaro, L., Bosch, J., 1998. Pharmacological treatment of portal hypertension: an evidence-based approach, Seminars in liver disease, pp. 475-505.

Doadrio, A.L., Doadrio, J.C., Sánchez-Montero, J.M., Salinas, A.J., Vallet-Regí, M., 2010. A rational explanation of the vancomycin release from SBA-15 and its derivative by molecular modelling. Microporous and Mesoporous Materials 132, 559-566.

Doadrio, A.L., Salinas, A.J., Sánchez-Montero, J.M., Vallet-Regí, M., 2015. Drug release from ordered mesoporous silicas. Current Pharmaceutical Design 21, 6213-6819.

Doadrio, A.L., Sánchez-Montero, J.M., Doadrio, J.C., Salinas, A.J., Vallet-Regí, M., 2014. A molecular model to explain the controlled release from SBA-15 functionalized with APTES. Microporous and Mesoporous Materials 195, 43-49.

DrugBank. http://www.drugbank.ca/ (accessed 1 June 2016).

European Society of Cardiology. Arterial hypertension guidelines. http://www.escardio.org/Guidelines-&-Education/Clinical-Practice-Guidelines/Arterial-Hypertension-Management-of (accessed 1 June 2016).

Exaire-Murad, E., Fern, L., Aldrete-Velasco, J.A., Nuntilde, E.I., Garcia, J.G.R., Flores-Murrieta, F.J., del Carmen Carrasco-Portugal, M., Santos-Caballero, N., 2015. Comparison of the efficacy and safety of an oral combination of losartan, hydrochlorothiazide and simvastatin against separated components, in hypertensive and dyslipidemic patients. African Journal of Pharmacy and Pharmacology 9, 484-491.

Ford, E.S., Ajani, U.A., Croft, J.B., Critchley, J.A., Labarthe, D.R., Kottke, T.E., Giles, W.H., Capewell, S., 2007. Explaining the decrease in US deaths from coronary disease, 1980–2000. New England Journal of Medicine 356, 2388-2398.

Gadepalli, S.G., Deme, P., Kuncha, M., Sistla, R., 2014. Simultaneous determination of amlodipine, valsartan and hydrochlorothiazide by LC–ESI-MS/MS and its application to pharmacokinetics in rats. Journal of Pharmaceutical Analysis 4, 399-406.

Gordon, T., Castelli, W.P., Hjortland, M.C., Kannel, W.B., Dawber, T.R., 1977. High density lipoprotein as a protective factor against coronary heart disease: the Framingham Study. The American journal of medicine 62, 707-714.

He, Y., Seaton, N.A., 2003. Experimental and Computer Simulation Studies of the Adsorption of Ethane, Carbon Dioxide, and Their Binary Mixtures in MCM-41. Langmuir 19, 10132-10138.

Higuchi, T., 1963. Mechanism of sustained-action medication. Theoretical analysis of rate of release of solid drugs dispersed in solid matrices. Journal of pharmaceutical sciences 52, 1145-1149.

Izquierdo-Barba, I., Colilla, M., Manzano, M., Vallet-Regí, M., 2010. *In vitro* stability of SBA-15 under physiological conditions. Microporous and Mesoporous Materials 132, 442-452.

Jamerson, K., Weber, M.A., Bakris, G.L., Dahlöf, B., Pitt, B., Shi, V., Hester, A., Gupte, J., Gatlin, M., Velazquez, E.J., 2008. Benazepril plus amlodipine or hydrochlorothiazide for hypertension in high-risk patients. New England Journal of Medicine 359, 2417-2428.

James, P.A., Oparil, S., Carter, B.L., Cushman, W.C., Dennison-Himmelfarb, C., Handler, J., Lackland, D.T., LeFevre, M.L., MacKenzie, T.D., Ogedegbe, O., 2014. 2014 evidence-based guideline for the management of high blood pressure in adults: report from the panel members appointed to the Eighth Joint National Committee (JNC 8). Jama 311, 507-520.

Kannel, W.B., McGee, D.L., 1979. Diabetes and cardiovascular disease: The framingham study. JAMA 241, 2035-2038.

Katsiki, N., Athyros, V.G., Karagiannis, A., 2013. Single-pill combinations: a therapeutic option or necessity for vascular risk treatment? Journal of Drug Assessment 2, 67-71.

Knežević, N.Ž., Ruiz-Hernández, E., Hennink, W.E., Vallet-Regí, M., 2013. Magnetic mesoporous silica-based core/shell nanoparticles for biomedical applications. RSC Advances 3, 9584-9593.

Lonn, E., Bosch, J., Teo, K.K., Pais, P., Xavier, D., Yusuf, S., 2010. The polypill in the prevention of cardiovascular diseases key concepts, current status, challenges, and future directions. Circulation 122, 2078-2088.

MacMahon, S., Peto, R., Collins, R., Godwin, J., Cutler, J., Sorlie, P., Abbott, R., Neaton, J., Dyer, A., Stamler, J., 1990. Blood pressure, stroke, and coronary heart disease: part 1, prolonged differences in blood pressure: prospective observational studies corrected for the regression dilution bias. The Lancet 335, 765-774.

Mitchell, G.F., Hwang, S.-J., Vasan, R.S., Larson, M.G., Pencina, M.J., Hamburg, N.M., Vita, J.A., Levy, D., Benjamin, E.J., 2010. Arterial Stiffness and Cardiovascular Events: The Framingham Heart Study. Circulation 121, 505-511.

Morris, G.M., Goodsell, D.S., Halliday, R.S., Huey, R., Hart, W.E., Belew, R.K., Olson, A.J., 1998. Automated docking using a Lamarckian genetic algorithm and an empirical binding free energy function. Journal of Computational Chemistry 19, 1639-1662.

Petrelli, A., Valabrega, G., 2009. Multitarget drugs: the present and the future of cancer therapy.

PubChem. https://pubchem.ncbi.nlm.nih.gov/search/ - collection=compounds (accessed 1 June 2016).

Ritger, P.L., Peppas, N.A., 1987. A simple equation for description of solute release I. Fickian and non-fickian release from non-swellable devices in the form of slabs, spheres, cylinders or discs. Journal of Controlled Release 5, 23-36.

Ruiz-Hernandez, E., Baeza, A., Vallet-Regí, M.a., 2011. Smart drug delivery through DNA/magnetic nanoparticle gates. ACS nano 5, 1259-1266.

Sleight, P., Pouleur, H., Zannad, F., 2006. Benefits, challenges, and registerability of the polypill. European heart journal 27, 1651-1656.

Slowing, I.I., Vivero-Escoto, J.L., Wu, C.-W., Lin, V.S.-Y., 2008. Mesoporous silica nanoparticles as controlled release drug delivery and gene transfection carriers. Advanced drug delivery reviews 60, 1278-1288.

Stöber, W., Fink, A., Bohn, E., 1968. Controlled growth of monodisperse silica spheres in the micron size range. Journal of colloid and interface science 26, 62-69.

Study, T.I.P., 2009. Effects of a polypill (Polycap) on risk factors in middle-aged individuals without cardiovascular disease (TIPS): a phase II, double-blind, randomised trial. The Lancet 373, 1341-1351.

Tang, F., Li, L., Chen, D., 2012. Mesoporous silica nanoparticles: synthesis, biocompatibility and drug delivery. Advanced Materials 24, 1504-1534.

Ugliengo, P., Sodupe, M., Musso, F., Bush, I.J., Orlando, R., Dovesi, R., 2008. Realistic Models of Hydroxylated Amorphous Silica Surfaces and MCM-41 Mesoporous Material Simulated by Large-scale Periodic B3LYP Calculations. Advanced Materials 20, 4579-4583.

Vallet-Regí, M., Balas, F., Arcos, D., 2007. Mesoporous materials for drug delivery. Angewandte Chemie International Edition 46, 7548-7558.

Vallet-Regi, M., Rámila, A., del Real, R.P., Pérez-Pariente, J., 2001. A New Property of MCM-41: Drug Delivery System. Chemistry of Materials 13, 308-311.

Wald, D.S., Morris, J.K., Wald, N.J., 2012. Randomized polypill crossover trial in people aged 50 and over. PLoS One 7, e41297.

Wald, N.J., Law, M.R., 2003. A strategy to reduce cardiovascular disease by more than 80%. Bmj 326, 1419.

Williams, C.D., Travis, K.P., Burton, N.A., Harding, J.H., 2016. A new method for the generation of realistic atomistic models of siliceous MCM-41. Microporous and Mesoporous Materials 228, 215-223.

Wilson, P.W.F., D'Agostino, R.B., Levy, D., Belanger, A.M., Silbershatz, H., Kannel, W.B., 1998. Prediction of Coronary Heart Disease Using Risk Factor Categories. Circulation 97, 1837-1847.

Yang, P., Gai, S., Lin, J., 2012. Functionalized mesoporous silica materials for controlled drug delivery. Chemical Society Reviews 41, 3679-3698.

Yusuf, S., 2002. Two decades of progress in preventing vascular disease. The Lancet 360, 2-3.

Zhuo, S., Huang, Y., Hu, J., Liu, H., Hu, Y., Jiang, J., 2008. Computer Simulation for Adsorption of CO 2, N 2 and Flue Gas in a Mimetic MCM-41. The Journal of Physical Chemistry C 112, 11295-11300.

Table 1. HPLC concentration gradient in acetonitrile (A)/Sörensen buffer at pH 3.5 (B).

Step	Time (min)	%A	%B
1	0	40	60
2	5	40	60
3	5.1	60	40
4	25	60	40
5	25.1	40	60

Table 2. Area, volume, PSA and DM for MCM-41 model and HTZ, AML, LS and SV from molecular modelling obtained by Spartan´14 software.

	Area ($Å^2$)	**Volume ($Å^3$)**	**PSA ($Å^2$)**	**DM (debye)**
MCM-41 model	3131.9	3042.1	2074.6	95.69
HZT	246.4	216.3	119.9	9.15
AML	432.3	401.6	81.4	1.67
LS	442.6	416.3	81.1	3.31
SV	468.2	452.8	59.1	3.10

Table 3. Kinetic data of 1 to 4 samples: HZT-MSN-41, AML-MSN-41, LS-MSN-41, SV-MSN-41.

	HZT-MSN-41	**AML-MSN-41**	**LS-MSN-41**	**SV-MSN-41**
n	0.49	0.41	0.31	0.23
K_{obs} (min^{-1})	0.51	0.0016	0.001	0.0044
R^2	0.956	0.981	0.981	0.957
t_{max} (min)	1920	2880	10200	2880
$\%D_{max}$	0.67	12.78	0.85	0.038
$\%D_5$	80.5	6.6	3.3	6.0

Table 4. Kinetic data of the components of polypill-MSN-41 (sample 5).

	HTZ	**AML**	**LS**	**SV**
n	0.03	0.40	0.27	0.47
K_{obs} (min^{-1})	0.49	0.0011	0.0022	0.0017
R^2	0.958	0.995	0.983	0.966
t_{max} (min)	2880	5880	10200	2880
$\%D_{max}$	9.88	22.0	1.10	0.14
$\%D_5$	82.9	2.6	1.6	3.5

FIGURE CAPTIONS

Fig 1. Morphology of MSN nanoparticles in sample 5 after releasing observed by SEM and TEM.

Fig 2. XRD patterns of MSN-41 and polypill-MSN-41 (sample 5). **Inside**: Adsorption-desorption isotherms of MSN-41 and polypill-MSN-41. D_p=diameter of pore; S_{BET}= BET surface area.

Fig 3. Best-fit curves from polypill-MSN-41 (sample 5) for each component and drugs-MSN-41 (samples 1 to 4) in comparative way. Percent release ($\%D_{(t)}$) was calculated for each drug loaded in MSN-41. For each drug and sample, the times indicated in the figure mean the starting of the drug degradation that supposed the end of the HPLC analysis.

Fig 4. a) Molecular modelling distances of MCM-41s model (3.81x2.1 nm). **b)** Docking results showing HTZ (white), AML (yellow), LS (blue), SV (pink) and MCM-41s. **c)** Electrostatic potential maps in a simulation way of HTZ, AML, LS and SV molecules on MCM-41s from Spartan´14 software. The color criteria represent negative charges in red and positive charges in blue.

Fig 5. Molecular modelling distances of MCM-41 new model (7.03x2.1 nm). **Left:** in length**. Right:** in diameter.

Figure(1)
Click here to download high resolution image

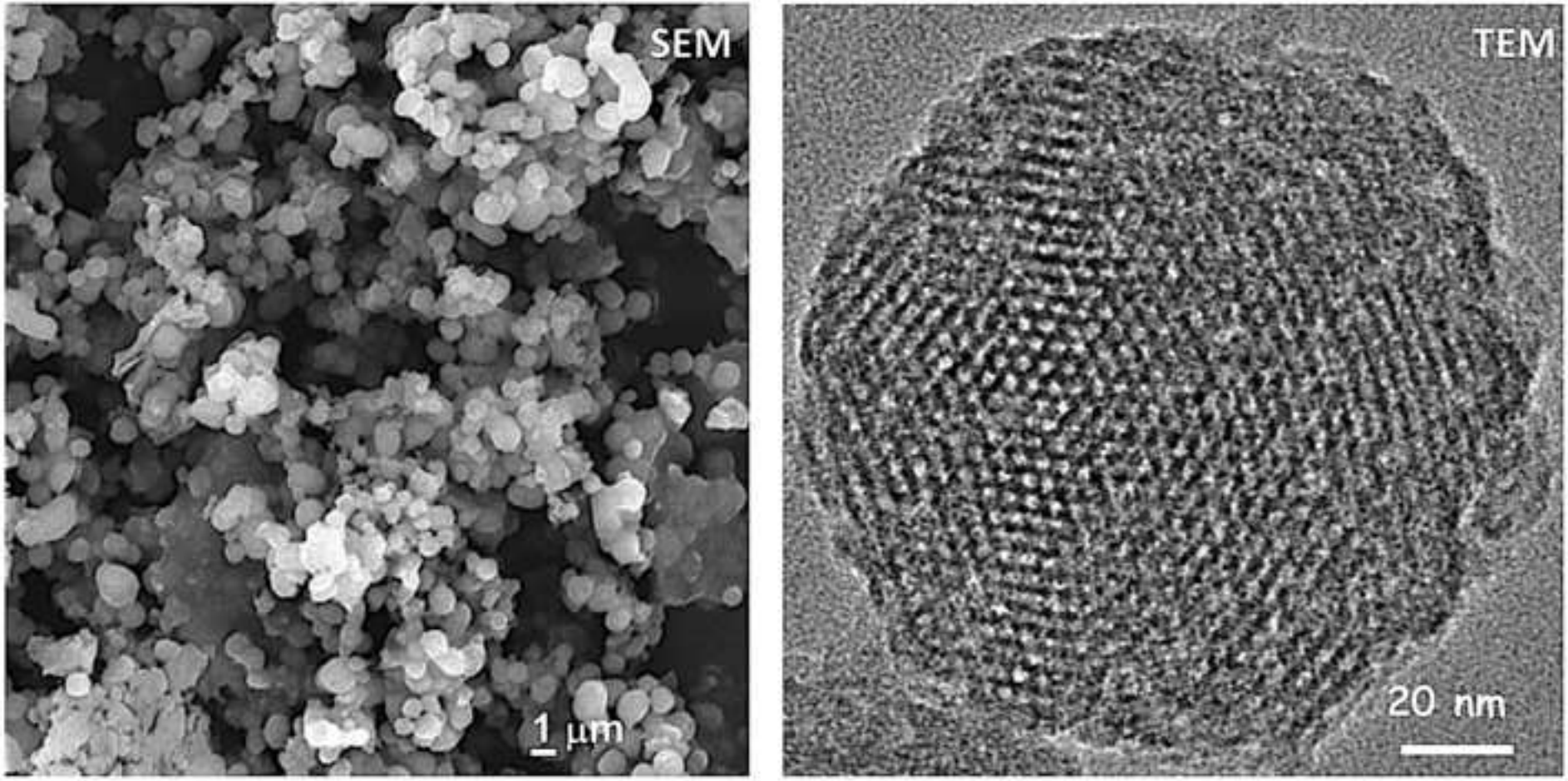

Figure(2)
Click here to download high resolution image

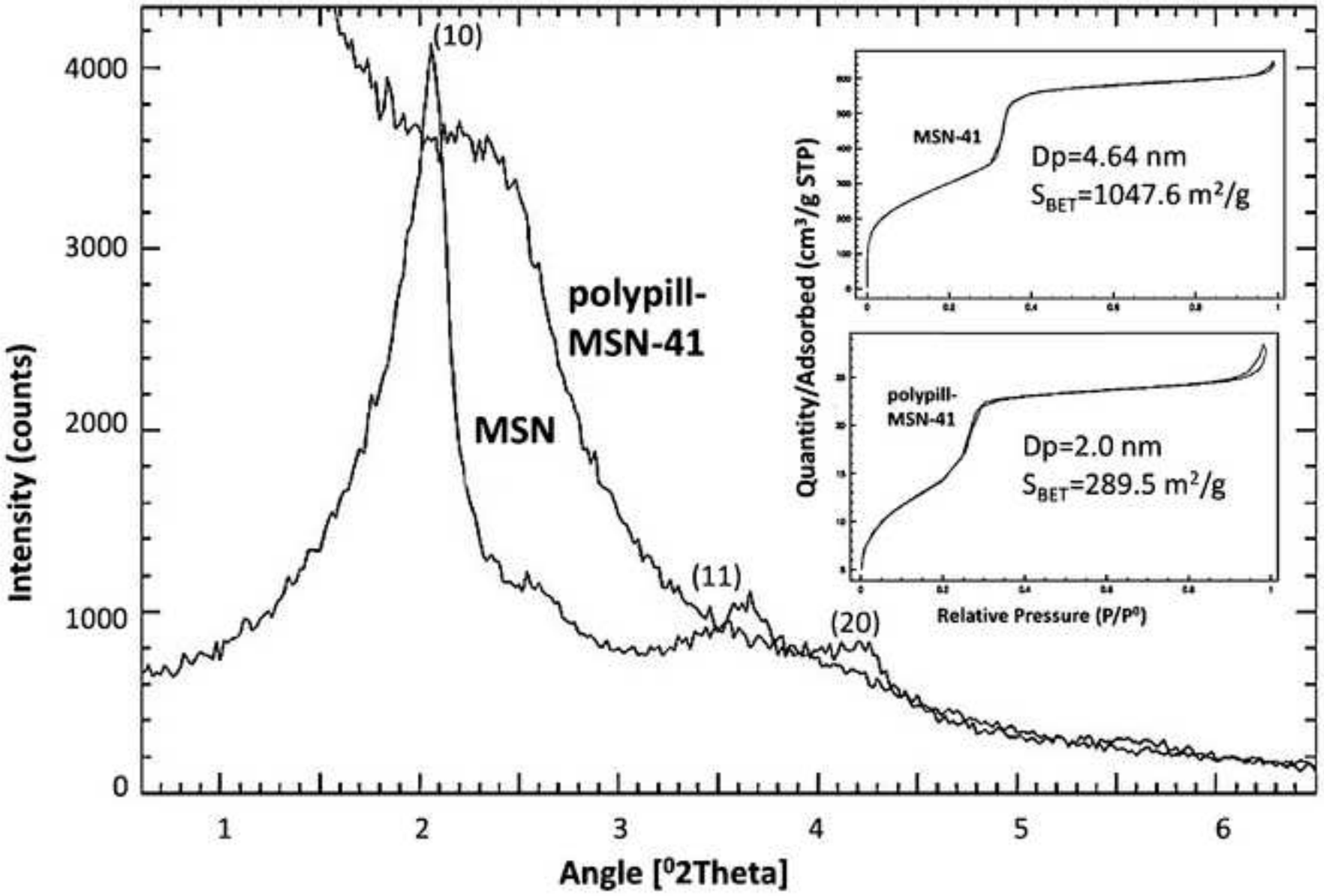

Figure(3)
Click here to download high resolution image

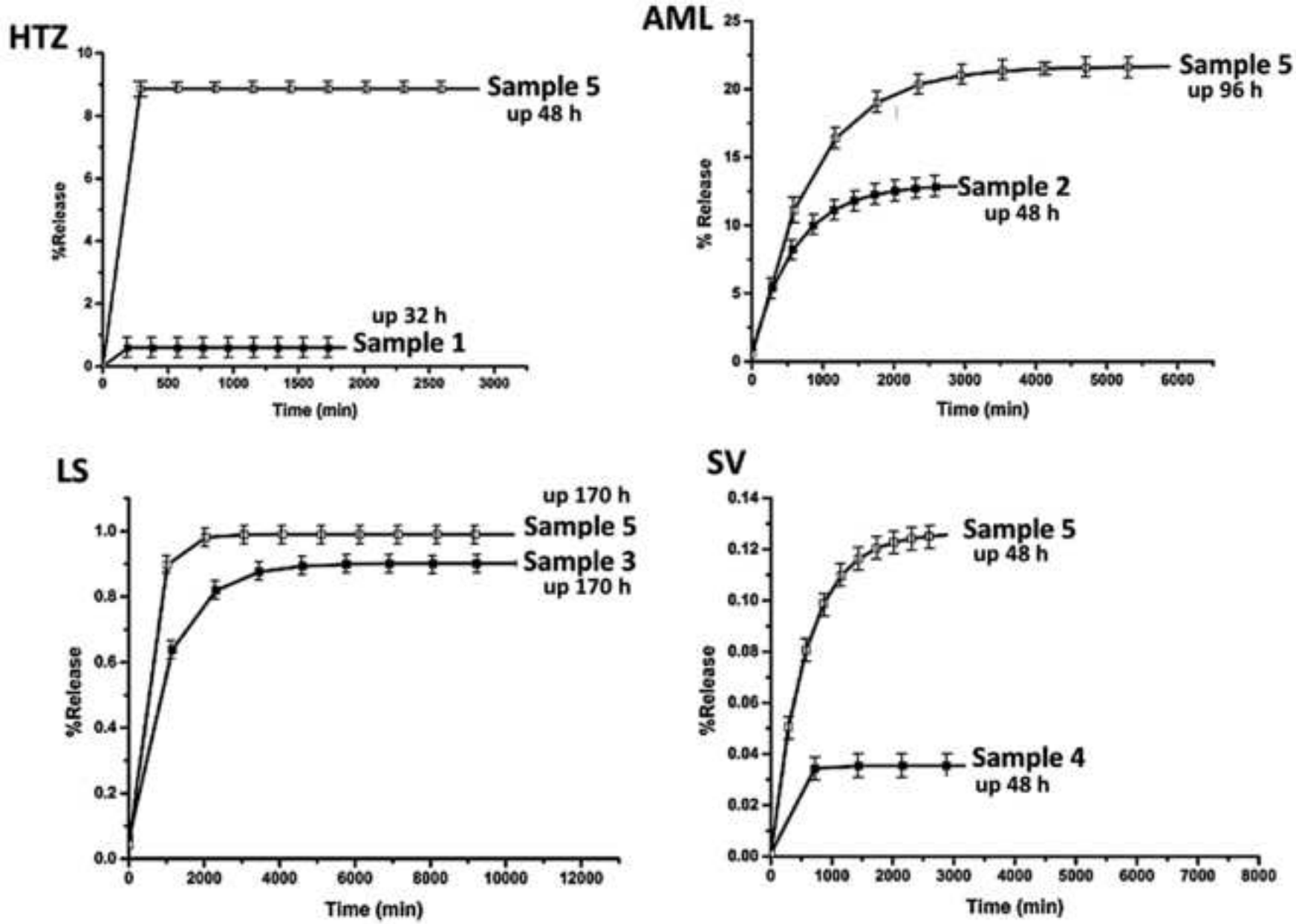

Figure(4)
Click here to download high resolution image

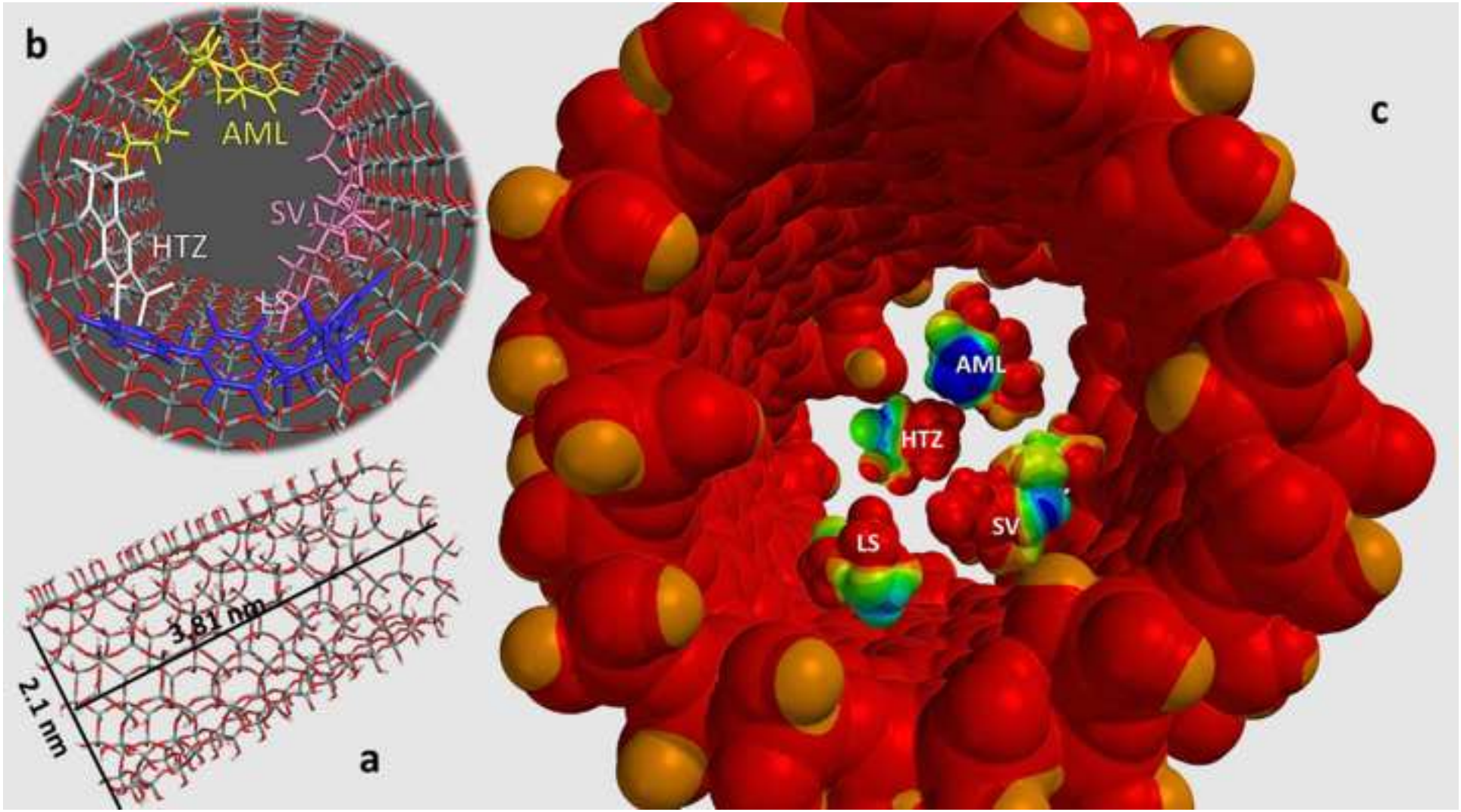

Figure(5)
Click here to download high resolution image